MRI Reveals Human Brown Adipose Tissue Is Rapidly Activated in Response to Cold

Stephan M. Oreskovich,[1,2] Frank J. Ong,[1] Basma A. Ahmed,[2,3] Norman B. Konyer,[4] Denis P. Blondin,[5] Elizabeth Gunn,[1,2] Nina P. Singh,[6] Michael D. Noseworthy,[4,7,8] Francois Haman,[9] Andre C. Carpentier,[10] Zubin Punthakee,[1,2,11] Gregory R. Steinberg,[2,3,11]* and Katherine M. Morrison[1,2]*

[1]Department of Pediatrics, McMaster University, Hamilton, Ontario L8S 4K1, Canada; [2]Centre for Metabolism, Obesity and Diabetes Research, McMaster University, Hamilton, Ontario L8S 4K1, Canada; [3]Department of Biochemistry and Biomedical Sciences, McMaster University, Hamilton, Ontario L8S 4K1, Canada; [4]Imaging Research Centre, St. Joseph's Healthcare, Hamilton, Ontario L8N 4A6, Canada; [5]Department of Pharmacology and Physiology, Faculty of Medicine and Health Sciences, Centre de Recherche du CHUS, Université de Sherbrooke, Sherbrooke, Quebec J1H 5N4, Canada; [6]Department of Radiology, McMaster University Medical Center, Hamilton, Ontario L8N 3Z5, Canada; [7]Department of Electrical and Computer Engineering, McMaster University, Hamilton, Ontario L8S 4K1, Canada; [8]McMaster School of Biomedical Engineering, McMaster University, Hamilton, Ontario L8S 4K1, Canada; [9]School of Human Kinetics, University of Ottawa, Ottawa, Ontario K1N 6N5, Canada; [10]Division of Endocrinology, Department of Medicine, Centre de Recherche du CHUS, Université de Sherbrooke, Sherbrooke, Quebec J1K 2R1, Canada; and [11]Division of Endocrinology and Metabolism, Department of Medicine, McMaster University, Hamilton, Ontario L8N 3Z5, Canada

ORCiD numbers: 0000-0002-1737-256X (K. M. Morrison).

*G.R.S. and K.M.M. contributed equally to this manuscript.

Context: In rodents, cold exposure induces the activation of brown adipose tissue (BAT) and the induction of intracellular triacylglycerol (TAG) lipolysis. However, in humans, the kinetics of supraclavicular (SCV) BAT activation and the potential importance of TAG stores remain poorly defined.

Objective: To determine the time course of BAT activation and changes in intracellular TAG using MRI assessment of the SCV (*i.e.,* BAT depot) and fat in the posterior neck region (*i.e.,* non-BAT).

Design: Cross-sectional.

Setting: Clinical research center.

Patients or Other Participants: Twelve healthy male volunteers aged 18 to 29 years [body mass index = 24.7 ± 2.8 kg/m^2 and body fat percentage = 25.0% ± 7.4% (both, mean ± SD)].

Intervention(s): Standardized whole-body cold exposure (180 minutes at 18°C) and immediate rewarming (30 minutes at 32°C).

Main Outcome Measure(s): Proton density fat fraction (PDFF) and T2* of the SCV and posterior neck fat pads. Acquisitions occurred at 5- to 15-minute intervals during cooling and subsequent warming.

Results: SCV PDFF declined significantly after only 10 minutes of cold exposure [−1.6% (SE: 0.44%; P = 0.007)] and continued to decline until 35 minutes, after which time it remained stable until 180 minutes. A similar time course was also observed for SCV T2*. In the posterior neck fat (non-BAT), there were no cold-induced changes in PDFF or T2*. Rewarming did not result in a change in SCV PDFF or T2*.

Conclusions: The rapid cold-induced decline in SCV PDFF suggests that in humans BAT is activated quickly in response to cold and that TAG is a primary substrate.

Abbreviations: ^{18}F-FDG, ^{18}F-fluorodeoxyglucose; BAT, brown adipose tissue; IDEAL, Iterative Decomposition with Echo-Asymmetry and Least squares estimation; PDFF, proton density fat fraction; PET, positron emission tomography; SAT, subcutaneous adipose tissue; SCV, supraclavicular; TAG, triacylglycerol.

Received 15 August 2019
Accepted 8 October 2019
First Published Online 14 October 2019

ISSN 2472-1972
December 2019 | Vol. 3, Iss. 12
doi: 10.1210/js.2019-00309 | Journal of the Endocrine Society | 2374–2384

Freeform/Key Words: brown adipose tissue, MRI, PDFF, T2*, cold exposure

Brown adipose tissue (BAT) contributes to nonshivering thermogenesis by catabolizing available substrates, including intracellular triacylglycerol (TAG) and blood glucose, through a futile cycle to generate heat [1, 2]. In adult humans, BAT is located predominantly in the supraclavicular (SCV) region and is activated by cold [3, 4]. Given its high-potential capacity for energy expenditure per gram of tissue, the role of BAT has been studied in the context of obesity and type 2 diabetes mellitus [5].

Intracellular TAG lipolysis is critical for cold-induced thermogenesis in human BAT [6]. However, the time course of this thermogenic activation is not well described, as commonly used methods to measure BAT metabolic activity, such as ^{18}F-fluorodeoxyglucose (^{18}F-FDG) positron emission tomography (PET) do not allow for serial measurements [7] and do not measure BAT thermogenesis *per se* [1]. Thus, alternative methodologies for assessing the time course of cold-induced BAT metabolic activity in humans are needed.

Chemical-shift MRI can offer insight into SCV BAT physiology through simultaneous mapping of proton density fat fraction (PDFF) and T2* relaxation time [8–17]. PDFF is the gold-standard in MRI-based biomarkers of tissue TAG concentration [18] and is accurately defined as the total density of mobile protons from fat relative to the total density of mobile protons from water. Because PDFF is based on the relative amounts of fat and water in a given region of interest, BAT-containing depots have consistently been shown to have a lower PDFF than white adipose tissue [9]. Importantly, when PDFF is measured using the Iterative Decomposition with Echo-Asymmetry and Least squares estimation (IDEAL)-IQ sequence, it is not susceptible to perfusion effects, thus providing an accurate measure of TAG content [19]. Consistent with changes in fatty acid metabolism in cold-activated BAT, recent studies have shown that SCV PDFF declines 0.4% to 2.2% in healthy adults [14, 15, 17]. PDFF in the SCV area was also previously correlated to ^{18}F-FDG uptake using PET-CT [17] and with the expression of uncoupling protein - 1 (UCP1) in both adults [20] and infants [21]. Therefore, reductions in SCV PDFF are an established measure of BAT metabolic activity; however, the time course for this reduction has not been clearly defined.

Increases in BAT metabolic activity are also associated with elevations in blood flow [22]. Therefore, assessing blood flow could offer insight into acute BAT activation. This can be achieved through evaluation of T2* relaxation time, a tissue-specific MRI property influenced by changes in blood flow, volume, and oxygenation during BAT activation [10, 15, 23]. T2* relaxation time correlates with ^{18}F-FDG uptake [10].

Given the capacity of SCV PDFF and T2* to dynamically assess BAT activity, our aim was to use a standardized, whole-body cold exposure protocol that has been used extensively to assess BAT metabolic activity with PET-CT [6, 24, 25], to assess SCV PDFF and T2* during cold exposure (*i.e.,* activation) and in subsequent rewarming, and to compare these findings with the subcutaneous fat in the posterior neck region (*i.e.,* a non-BAT adipose tissue). According to the time course identified in animal models [26, 27], we hypothesized that PDFF and T2* in the SCV region would change soon after the onset of cold exposure, but no changes in the posterior neck region would be seen. With rewarming, we expected to see a greater recovery in SCV T2* than in PDFF because the former measure responds temporally to brief repeated intervals of cooling and reheating [10].

1. Methods

A. Study Design and Population

Healthy adult men aged 18 to 29 years were recruited in Hamilton, ON, Canada, between July 2017 and February 2018. The study was approved by the Hamilton Integrated Research

Ethics Board, and participants provided informed written consent. Each participant completed two visits: Anthropometric and body composition measurements were completed at visit 1; the sequential cold and warm exposures with concurrent MRI imaging were completed at visit 2. Visits 1 and 2 occurred 10 to 30 days apart. To minimize environmental and nutritional influences on BAT activity, participants were asked to fast overnight and avoid caffeinated beverages for 12 hours, strenuous activity for 48 hours, and serotonin-rich foods (tomato, plum, kiwi, avocado, banana, pineapple, and walnuts) for 24 hours before both visits. Individuals taking adrenergic-acting medications and diabetes medications were excluded. A full list of the exclusion criteria can be found in an online repository [28].

B. Experimental Protocol

B-1. Visit 1

After confirmation of eligibility and completion of the consent process, anthropometric measurements were collected three times and an average was used. Weight (to the nearest 0.1 kg) was measured using an electronic platform scale (BMI Scale Model 882; Seca, Hamburg, Germany). Height (to the nearest 0.1 cm) was measured using a wall-mounted stadiometer (Height Measuring Rod Model 240; Seca, Hamburg, Germany). Body composition was measured using dual-energy X-ray absorptiometry (GE Lunar Prodigy Advance, Model 8743; GE Healthcare, Mississauga, Ontario, Canada). Men with a body fat percentage >25% were considered to have excessive adiposity [29, 30]. All dual-energy X-ray absorptiometry scans were reviewed (by K.M.M.) to ensure accurate delineation of the standardized regions of interest.

B-2. Visit 2

Participants arrived for their MRI examination between 0745 and 1000 hours (Fig. 1). After a 30-minute acclimation period at room temperature (mean ± SD: 21.5°C ± 0.7°C) while wearing standardized clothing (light sleeveless *t*-shirt and shorts), participants changed into a standard liquid-conditioned suit (two-piece; Allen-Vanguard, Ottawa, ON, Canada) and were instructed to lie in a supine position on the MRI scanning table. Consistent with a robust cooling protocol known to adequately stimulate BAT [24], water was precooled and maintained at 18°C using a temperature- and flow-controlled water bath (IsoTemp 6200R28; Fisher Scientific, Ottawa, ON, Canada) and delivered to the suit via insulated tubing extensions for up to 180 minutes. Immediately after cold exposure, the same water-perfused cooling garment was connected to a separate water bath set at 32°C (VWR, Avantor, Radnor, PA) for 30 minutes.

For participants 1 and 2, MRI scans were acquired at 5-minute intervals for the first 15 and 30 minutes, respectively, and at 15-minute intervals for the remainder of the cold exposure. After preliminary review of the data, it was decided to obtain PDFF measures every 5 minutes for the first 60 minutes of cold exposure and then every 15 minutes until the end of

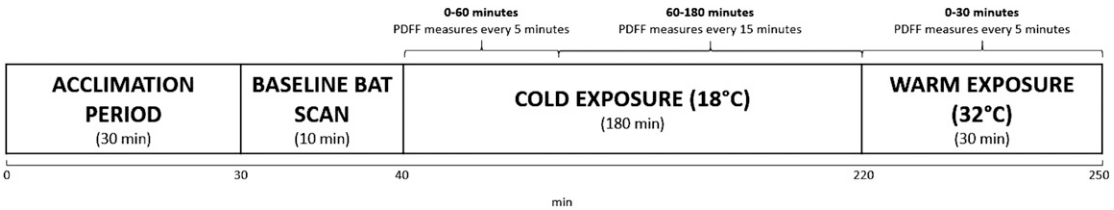

Figure 1: Timeline of cold exposure and MRI imaging (visit 2). After a 30-min acclimation period at room temperature, the participant donned the two-piece water-perfused suit and entered the MRI room. Cooling began immediately after a baseline neck scan, and MRI measures were obtained every 5 min during the first 60 min of cooling and every 15 min thereafter. Scans were obtained every 5 min during the subsequent 30-min warm exposure.

cold exposure for the remaining participants. For all participants, scans were acquired every 5 minutes during the subsequent warming phase.

Primary outcome of the study: PDFF. BAT activity, the primary outcome of this study, was quantified as change in PDFF from baseline to each time point. This was calculated as PDFF at a specific time point minus PDFF at baseline, whereby a negative result indicated a reduction in PDFF.

Secondary outcome of the study: T2.* Change in the T2* was calculated in a similar manner and was considered a measure of change in tissue perfusion.

C. Quantification of SCV Adipose Tissue Fat Fraction

C-1. MRI acquisition and segmentation of the SCV region

All MRI scans were performed using the same 3-Tesla whole-body MRI scanner (Discovery 750; GE Healthcare, Waukesha, WI) located in the Imaging Research Centre at St. Joseph's Healthcare Hamilton. BAT MRI scans were acquired via the IDEAL-IQ sequence in the axial plane using a head/neck/spine array coil. IDEAL-IQ is a commercially available three-dimensional gradient multiecho MRI sequence that provides an accurate and unconfounded measure of mobile tissue TAG content by accounting for T2* decay (*i.e.,* perfusion) and the multiple spectral peaks of fat [31]. This pulse sequence generates six distinct image contrasts: water-only, fat-only, in-phase, out-of-phase, PDFF, and R2* images. R2* images were transformed from T2* images (T2* = 1/R2*). To ensure that the entire neck and the SCV region were captured, image acquisition started at the C2/C3 disk and ended at the T4/T5 disk. Specific MRI protocol parameters are presented in an online repository [28].

Image analysis was performed using Analyze Pro (Version 1; Mayo Clinic, Biomedical Imaging Resource, AnalyzeDirect, Overland Park, KS). All adipose tissue bound by the sternocleidomastoid medially, trapezius posteriorly, and clavicle inferiorly at each of the axial slices between the C5-C6 and T1-T2 disks were manually segmented [32]. Because the SCV region is heterogeneous in morphology, a 30% to 100% PDFF range was applied to exclude nonadipose tissues [8]. On the basis of a report that human tissue with a T2* value <26 ms consisted mostly of muscle, fluid, or white adipocytes [8] and that the IDEAL-IQ sequence does not accurately detect voxels below T2* = 2 ms, an additional T2* window between 2 and 25 ms was used to help isolate BAT from white adipose tissues. Further, the outer border of each region of interest (*i.e.,* 1 × 3 voxels) was excluded to mitigate any inherent partial volume effects. All image voxels that remained after application of these criteria were considered to be SCV BAT (Fig. 2) and were summed to produce average PDFF % and T2* values for each scan (*i.e.,* time point).

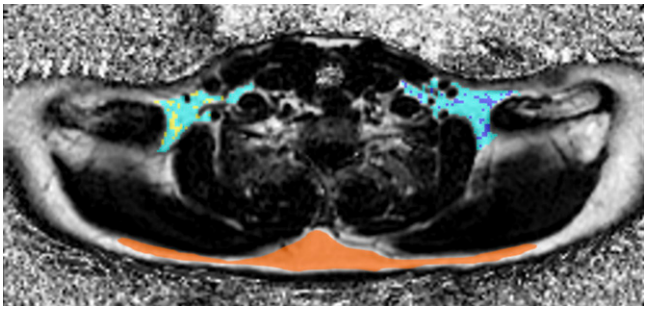

Figure 2. MRI representative axial PDFF map at the C7/T1 disk space. Voxels marked in teal were considered to be SCV BAT as their calculated PDFF and T2* values fell within the threshold criteria. Those marked in blue and yellow fell within the PDFF threshold but not the T2* threshold and were excluded from further analysis. Voxels marked in orange were identified as posterior neck subcutaneous adipose tissue.

Scans of subcutaneous adipose tissue (SAT) in the posterior neck region, not typically associated with cold-induced thermogenesis in adult humans, were performed in parallel with BAT [33]. The same PDFF and T2* windows were used for this tissue depot as for SCV BAT; however, segmentation was restricted to any SAT posterior to the trapezius at the C5-C6, C6-C7, and C7-T1 vertebral disk spaces exclusively, consistent with previous reports [12, 15, 34] (Fig. 2).

Inlet-outlet temperatures. Two fiber-optic temperature probes (FO Temp Sensor, Polymide Tip, Neoptix; Qualitrol, Quebec, Canada) were fixed to the tubing-suit interface (*i.e.,* manifold system). Inlet (*i.e.,* water delivered to the suit) and outlet (*i.e.,* water leaving the suit) temperatures were recorded using a data logger (Model RFX273A; Neoptix, Quebec, Canada) at 15-second intervals during the cooling and warming periods.

Environmental factors. The temperature inside the MRI scanning room, as measured by the MRI system and displayed on the MRI console, was recorded every 30 minutes. There were no deviations greater than ±0.5°C from the baseline-recorded temperature; therefore, only the first recorded value was used for analysis. To determine the influence of outdoor temperature on MRI findings, the average outdoor temperature 1 hour before visit 2 was obtained from data collected by the McMaster University Weather Station (http://geomedia.mcmaster.ca/muws/archives.html).

D. Statistical Analysis

The sample size was based on a previous report by Blondin *et al.* [35] in which inclusion of six participants conferred a power of >80% to detect a significant cold-induced effect on BAT activity (two-tailed test; $\alpha = 0.05$) with the same cooling protocol and in a similar cohort of males, albeit using PET-CT as the imaging modality. Pairwise comparisons using a random-slope linear mixed model with PDFF change as the dependent variable, time as the independent variable, and measures at either 0 (for SCV BAT and posterior neck SAT) or 180 minutes (for SCV BAT only) as the reference values were used to identify time points of significant change in PDFF during the time course. A linear mixed model with a first-order autoregressive repeated covariance structure (*i.e.,* model that provided the lowest absolute Bayesian information criteria value [36, 37]) was selected for this analysis because it is robust against missing data and unequal time intervals [38]. The same analyses were repeated using change in T2* relaxation time from baseline as the dependent variable. Demographic, anthropometric, and environmental characteristics of those who did and did not complete the 180-minute cold exposure were compared using independent samples *t* tests. Analyses were performed using Microsoft Excel©, SPSS Statistics (version 23), and GraphPad Prism (version 7). A P value of <0.05 using a two-tailed test was considered statistically significant. Values are expressed as mean (SD) for normally distributed data and as median (Q1, Q3) for skewed data.

2. Results

Of the 40 potential participants who expressed interest in the study, 26 declined participation, two were deemed ineligible after initial screening because of use of excluded medications, and 12 were enrolled. The characteristics of the 12 participants who were enrolled in the study are presented in Table 1. All 12 of the enrolled participants completed at least 60 minutes of cold exposure, and seven completed the full 180 minutes. Six participants were classified as overweight [body mass index (BMI) ≥ 25.0 kg/m^2], and of these, four had >25% total body fat. Of the six participants with a normal BMI, one had >25% total body fat. Those who completed the 180-minute cold exposure (*i.e.,* completers) did not differ in age, percentage of body fat, or BMI from those who did not complete (*i.e.,* noncompleters), and there were no differences between groups in the environmental conditions on the day of study

Table 1. Participant and Study Characteristics

Variable	All (n = 12)	Completers (n = 7)	Noncompleters (n = 5)	*P*
Participant characteristics				
Age, y	22.8 (2.6)	22.6 (3.0)	23.2 (2.2)	0.702
BMI, kg/m^2	24.7 (2.8)	24.5 (2.6)	25.1 (3.4)	0.720
Body fat, %	25.0 (7.4)	22.8 (6.0)	28.1 (8.8)	0.239
Time course MRI session				
Ambient temperature, °C[a]	20.3 (0.5)	20.1 (0.7)	20.4 (0.2)	0.417
Inlet temperature, °C[b]	18.9 (0.2)	18.9 [18.9, 19.0]	18.8 [18.7, 18.9]	—
ΔOutlet-inlet, °C[b]	3.5 (0.1)	3.5 [3.5, 3.6]	3.4 [3.4, 3.4]	—
Outdoor temperature, °C	2.9 (10.9)	4.5 (13.3)	0.6 (7.3)	0.549
BAT-specific characteristics				
PDFF reduction at 10 min	−1.6 (1.5)	−1.2 (1.1)	−2.2 (2.0)	0.266
PDFF reduction at 60 min	−3.0 (1.7)	−2.9 (1.2)	−3.2 (2.7)	0.776

Values are mean (SD) for normally distributed data or median [Q1, Q3] for nonnormal data. *P* values are for the comparisons of completers vs noncompleters by independent samples *t* test.
[a]n = 10 for all, n = 5 for completers, n = 5 for noncompleters, and n = 2 for not recorded.
[b]n = 6 for all, n = 4 for completers, n = 2 for noncompleters, n = 4 for lost to technical difficulties, and n = 2 for not recorded.

(Table 1). Further, the decline in PDFF from baseline to 60 minutes did not differ between completers and noncompleters (Table 1). The recorded air temperature inside the MRI room (range, 19.2°C to 21.0°C) and the $\Delta_{\text{Outlet-Inlet}}$ (range, 3.47°C to 3.67°C) were quite consistent, suggesting the intensity of the exposure condition was comparable across participants.

A. Changes in SCV BAT PDFF and T2 With Cooling Are Rapid*

All participants exhibited a measurable decrease in PDFF (Fig. 3A for grouped data; online repository for individualized data [28]). A significant reduction in PDFF from baseline was evident at 10 minutes after the onset of cold exposure [mean PDFF reduction at 10 minutes minus mean PDFF reduction at 0 minutes was −1.6% (SE: 0.44%; $P = 0.007$)]. At 35 minutes and beyond, reductions in PDFF did not differ from reduction after 180 minutes of cooling [mean PDFF reduction at 180 minutes minus mean PDFF reduction at 35 minutes was −1.3% (SE: 0.64%; $P > 0.100$)]. These findings were upheld when noncompleters were removed from the analysis (data not shown).

SCV BAT T2* relaxation time also decreased significantly by 10 minutes [mean T2* reduction at 10 minutes minus mean T2* reduction at 0 minutes was −0.54 ms (SE: 0.26 ms;

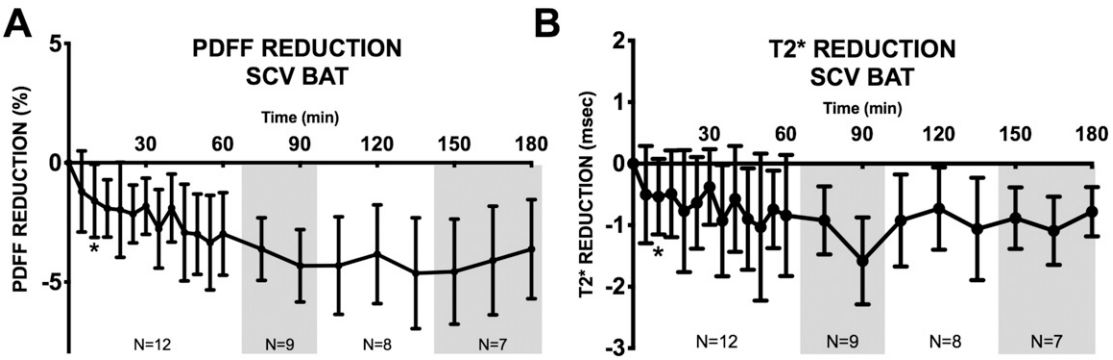

Figure 3. Cold exposure rapidly reduced SCV PDFF and T2*. (A) Time course plots of SCV PDFF and (B) T2* relaxation time throughout cooling. Reduction = measure at time point during cooling minus measure at baseline (time 0). Data are presented as mean ± SD. N for each time point is indicated on the figure background. *denotes the earliest point of significant change from baseline (via linear mixed model paired comparisons).

$P = 0.038$)]. The decline in T2* relaxation was not different from 180 minutes of cooling after only 5 minutes. This is consistent with a rapid, early change in blood flow. However, there was greater variability in the T2* measure at each time-point, making it less certain when the nadir change in T2* occurred in this population. (Fig. 3B for grouped data; online repository for individualized data [28]). These findings were also upheld when noncompleters were removed from the analysis (data not shown).

B. No Change in Posterior Neck PDFF With 3 Hours of Cooling

The change in posterior neck SAT PDFF during cooling is shown in Fig. 4. In contrast to the decline in PDFF seen in the SCV region, there were no statistically significant cold-induced declines in PDFF in this SAT depot. Similar results were found when noncompleters were removed (data not shown).

C. No Change in SCV BAT PDFF and T2 With 30 Minutes of Warming*

No differences between the final cold-induced time point and any subsequent SCV PDFF or T2* measurement during the 30-minute warming period were identified ($P > 0.05$ for all). Rather, SCV PDFF was maintained at or near the last measured cold-induced value (Fig. 5A and 5B). This was true when considering the entire cohort and the completers only.

3. Discussion

In the current study, we used a standardized, whole-body cold exposure protocol and acquired SCV PDFF measurements at frequent predefined intervals in healthy young men. Changes in SCV PDFF and T2* were rapid, as values decreased significantly in the first 10 minutes. Furthermore, after 35 and 5 minutes of cold, respectively, PDFF and T2* of the SCV region were not different from values obtained after 180 minutes of cold exposure. These findings provide insight into the time course of BAT activation and the potential role of TAG in BAT activation.

The rapid activation of BAT in response to cold seen in this study is consistent with results of other studies that evaluated BAT activation using other imaging modalities reflecting blood flow and oxygen saturation [10, 39]. Skin temperature in the SCV region, measured with infrared thermography, also increased within 10 minutes of cold exposure [40]. Leitner *et al.* [41] demonstrated that 20 minutes of cold exposure elicited an increase in BAT ^{18}F-FDG

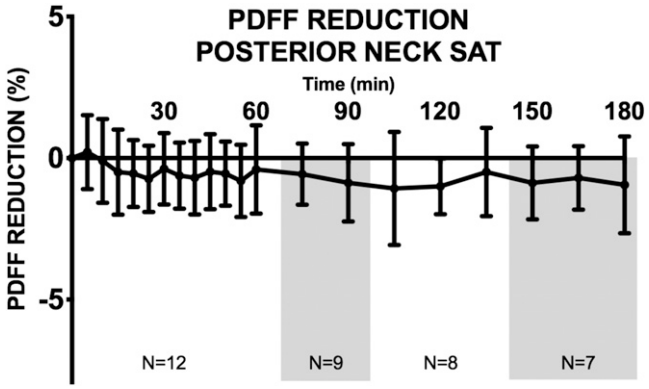

Figure 4. Time course plot of posterior neck SAT PDFF reduction throughout cooling. Reduction = measure at time point during cooling minus measure at baseline (time 0). Data are presented as mean ± SD. N for each time point is indicated on the figure background. No significant changes from baseline were found (via linear mixed model paired comparisons).

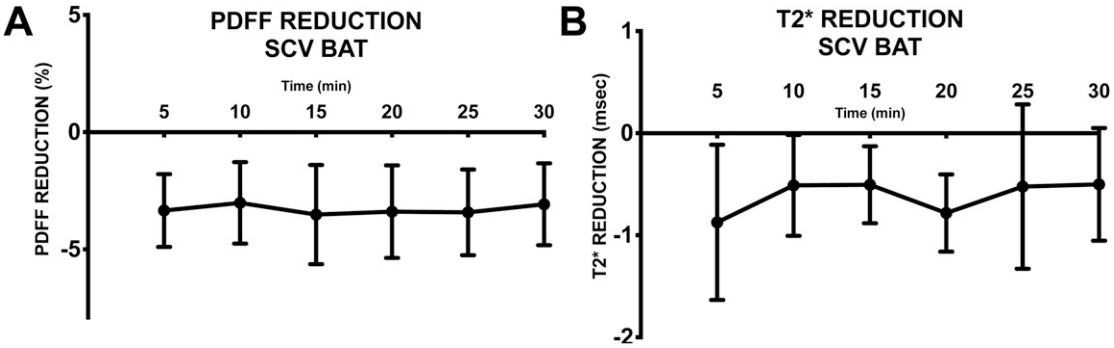

Figure 5. Time course plot of SCV BAT (A) PDFF and (B) T2* relaxation time reduction during warming. Reduction = measure at time point during warming minus measure at baseline (time 0). Data are presented as mean ± SD. N = 11 for each time point. No significant changes from the final cold-induced time point were found (via linear mixed model paired comparisons).

uptake similar to that at 60 minutes of cold exposure. Collectively, these data using distinct methodologies indicate that BAT activity in humans is rapidly increased in response to cold.

Our findings indicating a rapid decline in PDFF with cold exposure support the idea that TAG lipolysis in BAT is rapidly activated. These findings are consistent with those of Blondin *et al.* [6], who showed that pharmacological blockade of TAG lipolysis during cold exposure increased BAT glucose uptake and shivering, suggesting that TAG lipolysis is a primary substrate of cold-activated BAT. Because we found no further declines in BAT PDFF after 35 minutes, our data suggest that at this point in time the uptake of exogenous substrates (*e.g.,* circulating glucose, free fatty acids, or triglyceride lipoproteins) was sufficient to match the energetic demands of the activated BAT. Futures studies utilizing radiotracers are necessary to determine whether these substrates are directly oxidized or are incorporated into TAG before being oxidized.

Our study has limitations that warrant discussion. The rapid decline in T2* is consistent with rapid increases in BAT blood volume after sympathetic stimulation. This may have contributed to the initial reduction in PDFF; however, further declines in PDFF after 5 minutes are likely due to TAG lipolysis, consistent with the findings of previous investigators [15]. Restriction of our study to males under 30 years of age enabled us to analyze our results effectively using a smaller sample size, but we are unable to generalize our findings to females or to other age groups. Errors in PDFF may have been introduced, as the spatial resolution afforded by MRI is insufficient for differentiating between multiple cell types within a single voxel [11, 42, 43]. The temperature in the room where acclimation before cooling took place was slightly below thermoneutrality; therefore, cold-induced reductions in the SCV PDFF may have begun before the baseline MRI, resulting in underestimation of the cold-induced change in SCV PDFF [12]. We used T2* relaxation time to estimate tissue perfusion, but the IDEAL-IQ sequence parameters are optimized for precisely measuring PDFF and not T2* [23]; this may have affected the accuracy of our perfusion measurement.

In conclusion, in response to cold exposure, there were reductions in SCV PDFF and T2* within 10 and 5 minutes that were maintained for 180 minutes and were not affected by 30 minutes of rewarming. These findings suggest that a shorter duration of cold exposure than the 60- to 180-minute protocols commonly used would be sufficient to assess the activation of BAT. Future studies with larger populations and with a study population that is more diverse will be important in determining whether there is variability in this response.

Acknowledgments

We thank the members of the research team, Prasiddha Parthasarathy, and Emily Hutchings for their contributions and support in the research project. Computer server support was provided by the

laboratory of Dr. Andrew McArthur and the McMaster Service Laboratory and Repository. The authors thank all participants for their patience and commitment to research.

Financial Support: Funding for this study was provided by the Canadian Institutes of Health Research Programmatic Grants in Environment, Genes, and Chronic Diseases. G.R.S. is supported by a Canada Research Chair in Metabolism and Obesity and the J. Bruce Duncan Endowed Chair in Metabolic Diseases. A.C.C. holds the Canada Research Chair in Molecular Imaging of Diabetes.

Additional Information

Correspondence: Katherine M. Morrison, MD, 1280 Main Street West, HSC-3A, Hamilton, Ontario L8S 4K1, Canada. E-mail: kmorrison@mcmaster.ca.

Disclosure Summary: A.C.C. was the recipient of the GSK Chair in Diabetes of Université de Sherbrooke. The GlaxoSmithKline (GSK) Chair in Diabetes of the Université de Sherbrooke was created in part through a donation of $1 million by GSK to the Université de Sherbrooke. A.C.C. holds research funding from the Canadian Institutes of Health Research, Canadian Diabetes Association, Fonds de Recherche Québec – Santé, GSK, Merck, Pfizer, AstraZeneca, Aventis, Novo Nordisk, Eli Lilly, UniQure, and Caprion Biosciences. A.C.C. has participated in advisory boards for Amgen, UniQure, Merck, Janssen, Novo Nordisk, Novartis, HLS Therapeutics Inc., TVM Life Science Management, and AstraZeneca and made one conference sponsored by AstraZeneca. Z.P. has received honoraria for advice and speaking from Abbott, AstraZeneca/Bristol-Myers Squibb, Boehringer Ingelheim/Eli Lilly, Janssen, Merck, Novo Nordisk, Pfizer, and Sanofi. He has received research funds from Amgen, AstraZeneca/Bristol-Myers Squibb, Lexicon, Merck, Novo Nordisk, and Sanofi. G.R.S. holds research funding from the Canadian Institutes of Health Research and Diabetes Canada and is supported by a Canada Research Chair and the J. Bruce Duncan Endowed Chair in Metabolic Diseases. He has received research funding from Rigel Pharmaceuticals and Esperion Therapeutics and honoraria/consulting fees from AstraZeneca, Eli Lilly, Esperion Therapeutics, Novo Nordisk, Poxel, Pfizer, Merck, Rigel Pharmaceuticals, and Terns Pharmaceuticals. K.M.M. holds research funds from the Canadian Institutes of Health Research and has received funds from the Faculty of Health Sciences at McMaster University and the McMaster Children's Hospital Foundation. K.M.M. has participated on the advisory board of Akcea Therapeutics Canada Inc. The remaining authors have nothing to disclose.

Data Availability: De-identified data will be made available to interested investigators through direct contact with the corresponding author.

References and Notes

1. Carpentier AC, Blondin DP, Virtanen KA, Richard D, Haman F, Turcotte ÉE. Brown Adipose Tissue Energy Metabolism in Humans. *Front Endocrinol (Lausanne).* 2018;**9**:447.
2. Paulus A, van Marken Lichtenbelt W, Mottaghy FM, Bauwens M. Brown adipose tissue and lipid metabolism imaging. *Methods.* 2017;**130**:105–113.
3. Loh RKC, Kingwell BA, Carey AL. Human brown adipose tissue as a target for obesity management: beyond cold-induced thermogenesis. *Obes Rev.* 2017;**18**(11):1227–1242.
4. Ong FJ, Ahmed BA, Oreskovich SM, Blondin DP, Haq T, Konyer NB, Noseworthy MD, Haman F, Carpentier AC, Morrison KM, Steinberg GR. Recent advances in the detection of brown adipose tissue in adult humans: a review. *Clin Sci (Lond).* 2018;**132**(10):1039–1054.
5. Hanssen MJW, Hoeks J, Brans B, van der Lans AA, Schaart G, van den Driessche JJ, Jörgensen JA, Boekschoten MV, Hesselink MK, Havekes B, Kersten S, Mottaghy FM, van Marken Lichtenbelt WD, Schrauwen P. Short-term cold acclimation improves insulin sensitivity in patients with type 2 diabetes mellitus. *Nat Med.* 2015;**21**(8):863–865.
6. Blondin DP, Frisch F, Phoenix S, Guérin B, Turcotte ÉE, Haman F, Richard D, Carpentier AC. Inhibition of intracellular triglyceride lipolysis suppresses cold-induced brown adipose tissue metabolism and increases shivering in humans. *Cell Metab.* 2017;**25**(2):438–447.
7. van der Lans AAJJ, Wierts R, Vosselman MJ, Schrauwen P, Brans B, van Marken Lichtenbelt WD. Cold-activated brown adipose tissue in human adults: methodological issues. *Am J Physiol Regul Integr Comp Physiol.* 2014;**307**(2):R103–R113.
8. Hu HH, Perkins TG, Chia JM, Gilsanz V. Characterization of human brown adipose tissue by chemical-shift water-fat MRI. *AJR Am J Roentgenol.* 2013;**200**(1):177–183.

9. Franz D, Karampinos DC, Rummeny EJ, Souvatzoglou M, Beer AJ, Nekolla SG, Schwaiger M, Eiber M. Discrimination between brown and white adipose tissue using a 2-point Dixon water-fat separation method in simultaneous PET/MRI. *J Nucl Med*. 2015;**56**(11):1742–1747.
10. van Rooijen BD, van der Lans AAJJ, Brans B, Wildberger JE, Mottaghy FM, Schrauwen P, Backes WH, van Marken Lichtenbelt WD. Imaging cold-activated brown adipose tissue using dynamic T2*-weighted magnetic resonance imaging and 2-deoxy-2-[18F]fluoro-D-glucose positron emission tomography. *Invest Radiol*. 2013;**48**(10):708–714.
11. McCallister A, Zhang L, Burant A, Katz L, Branca RT. A pilot study on the correlation between fat fraction values and glucose uptake values in supraclavicular fat by simultaneous PET/MRI. *Magn Reson Med*. 2017;**78**(5):1922–1932.
12. Stahl V, Maier F, Freitag MT, Floca RO, Berger MC, Umathum R, Berriel Diaz M, Herzig S, Weber MA, Dimitrakopoulou-Strauss A, Rink K, Bachert P, Ladd ME, Nagel AM. *In vivo* assessment of cold stimulation effects on the fat fraction of brown adipose tissue using DIXON MRI. *J Magn Reson Imaging*. 2017;**45**(2):369–380.
13. Gashi G, Madoerin P, Maushart CI, Michel R, Senn JR, Bieri O, Betz MJ. MRI characteristics of supraclavicular brown adipose tissue in relation to cold-induced thermogenesis in healthy human adults. *J Magn Reson Imaging*. 2019;**50**(4):1160–1168.
14. Gifford A, Towse TF, Walker RC, Avison MJ, Welch EB. Characterizing active and inactive brown adipose tissue in adult humans using PET-CT and MR imaging. *Am J Physiol Endocrinol Metab*. 2016; **311**(1):E95–E104.
15. Lundström E, Strand R, Johansson L, Bergsten P, Ahlström H, Kullberg J. Magnetic resonance imaging cooling-reheating protocol indicates decreased fat fraction via lipid consumption in suspected brown adipose tissue. *PLoS One*. 2015;**10**(4):e0126705.
16. Deng J, Neff LM, Rubert NC, Zhang B, Shore RM, Samet JD, Nelson PC, Landsberg L. MRI characterization of brown adipose tissue under thermal challenges in normal weight, overweight, and obese young men. *J Magn Reson Imaging*. 2018; **47**(4):936–947.
17. Holstila M, Pesola M, Saari T, Koskensalo K, Raiko J, Borra RJ, Nuutila P, Parkkola R, Virtanen KA. MR signal-fat-fraction analysis and T2* weighted imaging measure BAT reliably on humans without cold exposure. *Metabolism*. 2017;**70**:23–30.
18. Caussy C, Reeder SB, Sirlin CB, Loomba R. Noninvasive, quantitative assessment of liver fat by MRI-PDFF as an endpoint in NASH trials. *Hepatology*. 2018;**68**(2):763–772.
19. Reeder SB, Hu HH, Sirlin CB. Proton density fat-fraction: a standardized MR-based biomarker of tissue fat concentration. *J Magn Reson Imaging*. 2012;**36**(5):1011–1014.
20. Reddy NL, Jones TA, Wayte SC, Adesanya O, Sankar S, Yeo YC, Tripathi G, McTernan PG, Randeva HS, Kumar S, Hutchinson CE, Barber TM. Identification of brown adipose tissue using MR imaging in a human adult with histological and immunohistochemical confirmation. *J Clin Endocrinol Metab*. 2014;**99**(1):E117–E121.
21. Hu HH, Tovar JP, Pavlova Z, Smith ML, Gilsanz V. Unequivocal identification of brown adipose tissue in a human infant. *J Magn Reson Imaging*. 2012;**35**(4):938–942.
22. U Din M, Raiko J, Saari T, Saunavaara V, Kudomi N, Solin O, Parkkola R, Nuutila P, Virtanen KA. Human brown fat radiodensity indicates underlying tissue composition and systemic metabolic health. *J Clin Endocrinol Metab*. 2017;**102**(7):2258–2267.
23. Franz D, Diefenbach MN, Treibel F, Weidlich D, Syväri J, Ruschke S, Wu M, Holzapfel C, Drabsch T, Baum T, Eggers H, Rummeny EJ, Hauner H, Karampinos DC. Differentiating supraclavicular from gluteal adipose tissue based on simultaneous PDFF and T_2 * mapping using a 20-echo gradient-echo acquisition. *J Magn Reson Imaging*. 2019;**50**(2):424–434.
24. Ouellet V, Labbé SM, Blondin DP, Phoenix S, Guérin B, Haman F, Turcotte EE, Richard D, Carpentier AC. Brown adipose tissue oxidative metabolism contributes to energy expenditure during acute cold exposure in humans. *J Clin Invest*. 2012;**122**(2):545–552.
25. Blondin DP, Labbé SM, Noll C, Kunach M, Phoenix S, Guérin B, Turcotte ÉE, Haman F, Richard D, Carpentier AC. Selective impairment of glucose but not fatty acid or oxidative metabolism in brown adipose tissue of subjects with type 2 diabetes. *Diabetes*. 2015;**64**(7):2388–2397.
26. Mottillo EP, Bloch AE, Leff T, Granneman JG. Lipolytic products activate peroxisome proliferator-activated receptor (PPAR) α and δ in brown adipocytes to match fatty acid oxidation with supply. *J Biol Chem*. 2012;**287**(30):25038–25048.
27. Branca RT, Zhang L, Warren WS, Auerbach E, Khanna A, Degan S, Ugurbil K, Maronpot R. *In vivo* noninvasive detection of Brown Adipose Tissue through intermolecular zero-quantum MRI. *PLoS One*. 2013;**8**(9):e74206.

28. Oreskovich SM, Ong FJ, Ahmed BA, Konyer NB, Blondin DP, Gunn E, Singh NP, Noseworthy MD, Haman F, Carpentier AC, Punthakee Z, Steinberg GR, Morrison KM. Data from: Magnetic resonance imaging reveals human brown adipose tissue is rapidly activated in response to cold. Dryad 2019. Deposited 21 October 2019. https://doi.org/10.5061/dryad.msbcc2ftd.
29. McArdle W, Katch F, Katch V. *Exercise Physiology: Nutrition, Energy, and Human Performance*. 4th ed. Baltimore, MD: Williams & Wilkins; 1996.
30. Physical Status: The Use and Interpretation of Anthropometry. Geneva, Switzerland: World Health Organization; 1995. WHO Technical Report Series 854.
31. Hu HH, Börnert P, Hernando D, Kellman P, Ma J, Reeder S, Sirlin C. ISMRM workshop on fat-water separation: insights, applications and progress in MRI. *Magn Reson Med*. 2012;**68**(2):378–388.
32. Hu HH, Yin L, Aggabao PC, Perkins TG, Chia JM, Gilsanz V. Comparison of brown and white adipose tissues in infants and children with chemical-shift-encoded water-fat MRI. *J Magn Reson Imaging*. 2013;**38**(4):885–896.
33. Sacks H, Symonds ME. Anatomical locations of human brown adipose tissue: functional relevance and implications in obesity and type 2 diabetes. *Diabetes*. 2013;**62**(6):1783–1790.
34. Franssens BT, Eikendal AL, Leiner T, van der Graaf Y, Visseren FLJ, Hoogduin JM. Reliability and agreement of adipose tissue fat fraction measurements with water-fat MRI in patients with manifest cardiovascular disease. *NMR Biomed*. 2016;**29**(1):48–56.
35. Blondin DP, Labbé SM, Tingelstad HC, Noll C, Kunach M, Phoenix S, Guérin B, Turcotte EE, Carpentier AC, Richard D, Haman F. Increased brown adipose tissue oxidative capacity in cold-acclimated humans. *J Clin Endocrinol Metab*. 2014;**99**(3):E438–E446.
36. Oberfeld D, Franke T. Evaluating the robustness of repeated measures analyses: the case of small sample sizes and nonnormal data. *Behav Res Methods*. 2013;**45**(3):792–812.
37. Vossoughi M, Ayatollahi SMT, Towhidi M, Ketabchi F. On summary measure analysis of linear trend repeated measures data: performance comparison with two competing methods. *BMC Med Res Methodol*. 2012;**12**:33.
38. Gueorguieva R, Krystal JH. Move over ANOVA: progress in analyzing repeated-measures data and its reflection in papers published in the *Archives of General Psychiatry*. *Arch Gen Psychiatry*. 2004;**61**(3):310–317.
39. Reber J, Willershäuser M, Karlas A, Paul-Yuan K, Diot G, Franz D, Fromme T, Ovsepian SV, Bézière N, Dubikovskaya E, Karampinos DC, Holzapfel C, Hauner H, Klingenspor M, Ntziachristos V. Non-invasive measurement of brown fat metabolism based on optoacoustic imaging of hemoglobin gradients. *Cell Metab*. 2018;**27**(3):689–701.e4.
40. Haq T, Crane JD, Kanji S, Gunn E, Tarnopolsky MA, Gerstein HC, Steinberg GR, Morrison KM. Optimizing the methodology for measuring supraclavicular skin temperature using infrared thermography: implications for measuring brown adipose tissue activity in humans. *Sci Rep*. 2017;**7**(1):11934.
41. Leitner BP, Weiner LS, Desir M, Kahn PA, Selen DJ, Tsang C, Kolodny GM, Cypess AM. Kinetics of human brown adipose tissue activation and deactivation. *Int J Obes (Lond)*. 2019;**43**(3):633–637.
42. Liu CY, McKenzie CA, Yu H, Brittain JH, Reeder SB. Fat quantification with IDEAL gradient echo imaging: correction of bias from T_1 and noise. *Magn Reson Med*. 2007;**58**(2):354–364.
43. Hu HH, Smith DL Jr, Nayak KS, Goran MI, Nagy TR. Identification of brown adipose tissue in mice with fat-water IDEAL-MRI. *J Magn Reson Imaging*. 2010;**31**(5):1195–1202.